Mapping the d−d Excited-State Manifolds of Transition Metal β-Diiminato−Imido Complexes. Comparison of Density Functional Theory and CASPT2 Energetics†

Abhik Ghosh,*,‡ Emmanuel Gonzalez,‡ Espen Tangen,‡ and Björn O. Roos*,§

Department of Chemistry, University of Tromsø, N-9037 Tromsø, Norway, and Department of Theoretical Chemistry, Chemical Center, University of Lund, P.O. Box 124, S-221 00 Lund, Sweden

Received: November 24, 2007; Revised Manuscript Received: February 8, 2008

Trigonal-planar, middle transition metal diiminato−imido complexes do not exhibit high-spin states, as might be naively expected on the basis of their low coordination numbers. Instead, the known Fe(III), Co(III), and Ni(III) complexes exhibit $S = {}^3/_2$, $S = 0$, and $S = {}^1/_2$ ground states, respectively. Kohn–Sham DFT calculations have provided a basic molecular orbital picture of these compounds as well as a qualitative rationale for the observed spin states. Reported herein are ab initio multiconfiguration second-order perturbation theory (CASPT2) calculations, which provide a relatively detailed picture of the d−d excited-state manifolds of these complexes. Thus, for a C_{2v} Fe^{III}(diiminato)(NPh) model complex, two near-degenerate states ($^4B_2$ and $^4B_1$) compete as contenders for the ground state. Moreover, the high-spin sextet, two additional quartets and even a low-spin doublet all occur at <0.5 eV, relative to the ground state. For the Co(III) system, although CASPT2 reproduces an $S = 0$ ground state, as observed experimentally for a related complex, the calculations also predict two exceedingly low-energy triplet states; there are, however, no other particularly low-energy d−d excited states. In contrast to the Fe(III) and Co(III) cases, the Ni(III) complex has a clearly nondegenerate $^2B_2$ ground state. The CASPT2 energetics provide benchmarks against which we can evaluate the performance of several common DFT methods. Although none of the functionals examined perform entirely satisfactorily, the B3LYP hybrid functional provides the best overall spin-state energetics.

Introduction

The electronic structures of low-coordinate first-row transition metal imido complexes may, at first glance, appear counterintuitive.[1] Thus, all known trigonal-planar[2] and pseudotetrahedral[3–5] Co(III)−imido complexes exhibit low-spin $S = 0$ ground states, which may seem at odds with their low coordination numbers. In the same vein, an Fe^{III}(nacnac)(NAd) (nacnac = β-diketiminato, Ad = 1-adamantyl) complex exhibits a relatively unusual $S = {}^3/_2$ ground state, as opposed to an $S = {}^5/_2$ one.[6] These developments, not surprisingly, have provided fertile ground for quantum chemical investigations and we have reported broad DFT studies of a number of transition metal imido complexes.[1,7–9] In this study, our goal is to deepen our appreciation of certain aspects of this area.

On the chemical front, we wish to extend our understanding of the diiminato−imido complexes beyond the basic description of bonding that is available for the electronic ground states. In other words, we are seeking a fairly accurate map of the excited-state energetics. Previous DFT calculations have hinted at the existence of multiple low-energy excited states for Fe(III) and Co(III) diiminato−imido complexes.[8] In addition, a ground-state singlet Co(III) hydrotris(pyrazolyl)borate−imido complex has actually been found to be a spin-crossover complex, with a low-energy paramagnetic excited state.[9,10] In the same vein, in contrast to the low-spin $S = ½$ states observed for Fe(III) trisphosphine−imido complexes,[1,7] a high-spin $S = {}^5/_2$ ground state has been predicted for an Fe(III) hydrotris(pyrazolyl)-borate−imido complex.[9] Stimulated by these findings, we embarked on a program to systematically map out the spin state energetics of Fe(III), Co(III) and Ni(III) diiminato−imido model complexes. The performance of DFT, regardless of the exchange-correlation functional, in such an endeavor seemed uncertain, at best.[11] Accordingly, we turned to *ab initio* multiconfiguration second-order perturbation theory (CASPT2)[12] to more reliably probe the excited-state manifolds of these compounds.

On the methodological side, the CASPT2 calculations allow us to examine the performance of a number of commonly used exchange-correlation functionals vis-à-vis the spin-state energetics of the compounds studied. As we and others have documented, this is a challenging problem for DFT and calibration studies against high-level *ab initio* calculations are still surprisingly rare.[13–15] The general impression on this matter seems to be that whereas classic pure functionals such as PW91,[16] BLYP,[17,18] and BP86[17,19] tend to favor lower-spin states, hybrid functionals, typified by B3LYP,[20–22] err in the opposite direction.[15] The CASPT2 calculations reported here, which should yield energies accurate to within 0.1–0.2 eV, have allowed us to test this generalization.

Methods

The metal complexes studied here (Figure 1) were all optimized with the OLYP[23] generalized gradient approximation (GGA), triple-ζ plus polarization Slater-type orbital basis sets, C_{2v} symmetry constraints,[24] a fine mesh for numerical integration of the matrix elements, and the ADF 2006 program system. [25] Subsequently, using the OLYP ground-state geometry, we carried out single-point calculations on a number of excited states using the following exchange-correlation functionals: OLYP, OPBE,[26,27] BLYP, PW91, BP86, B3LYP and B3LYP*.[28]

† Part of the "Sason S. Shaik Festschrift".

* Corresponding authors. E-mail: A.G., abhik@chem.uit.no.
‡ University of Tromsø.
§ University of Lund.

10.1021/jp711159h CCC: $40.75
Published on Web 04/24/2008

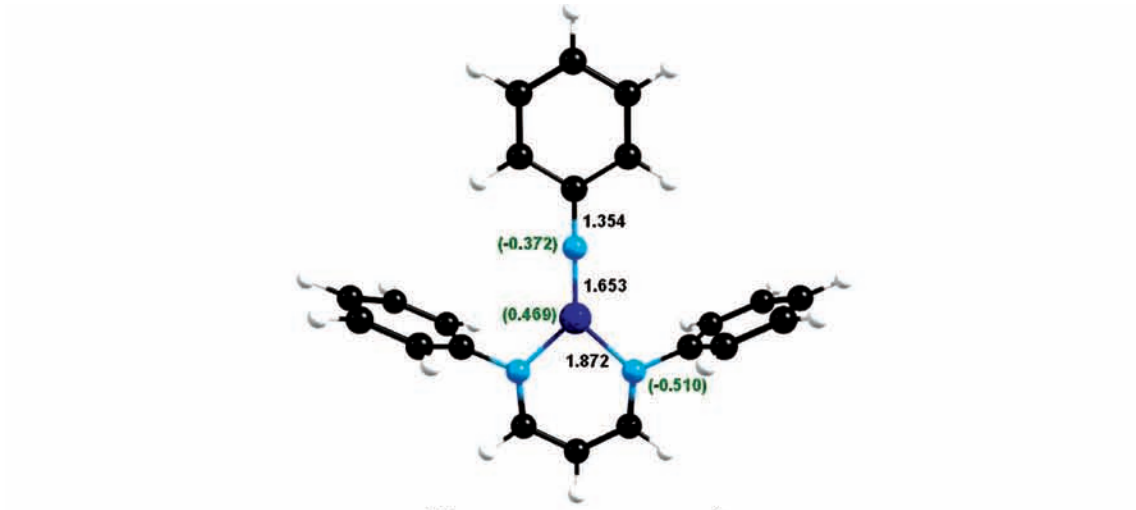

Co^{III}(diiminato)(NPh), $^2A_1$

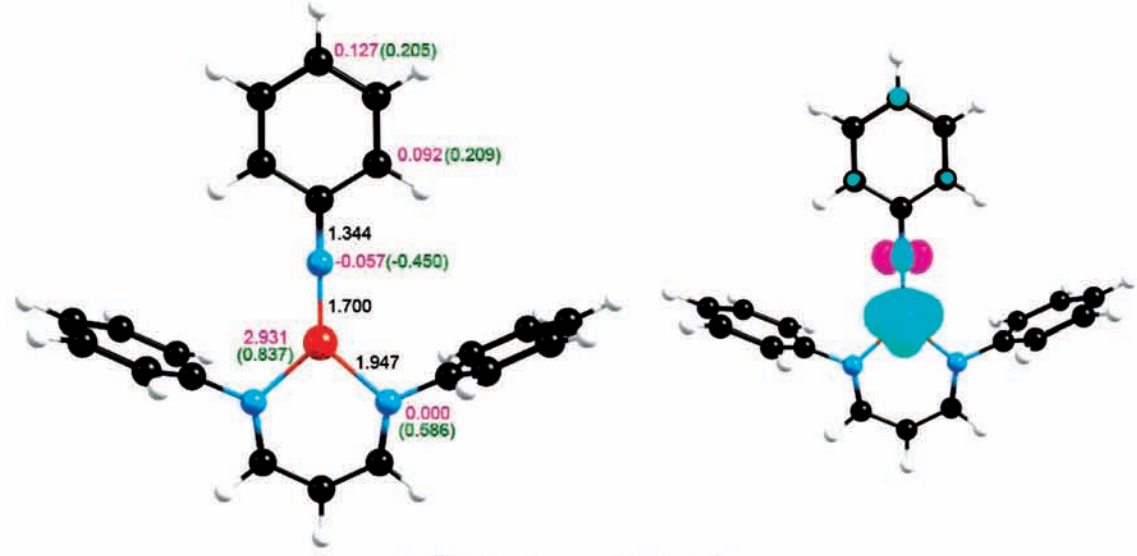

Fe^{III}(diiminato)(NPh), $^4B_2$

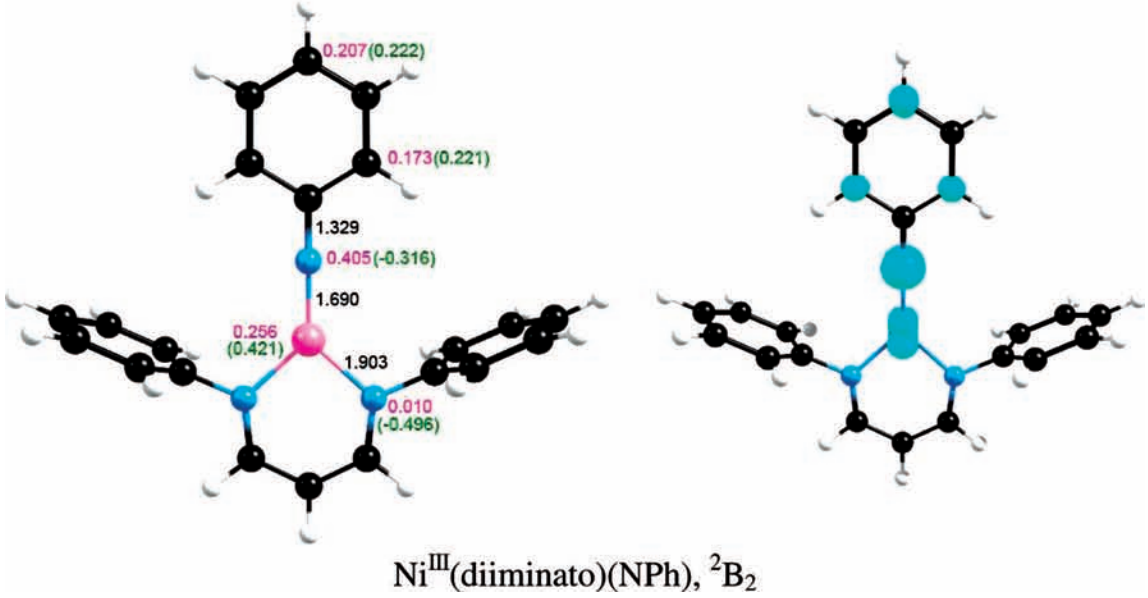

Ni^{III}(diiminato)(NPh), $^2B_2$

Figure 1. Selected OLYP/STO-TZP results for the ground states of the Fe(III), Co(III), and Ni(III) complexes studied: distances (Å, black), Mulliken charges (in parentheses, green), and spin populations (magenta). In the spin density plots, majority and minority spin densities are shown in cyan and magenta, respectively.

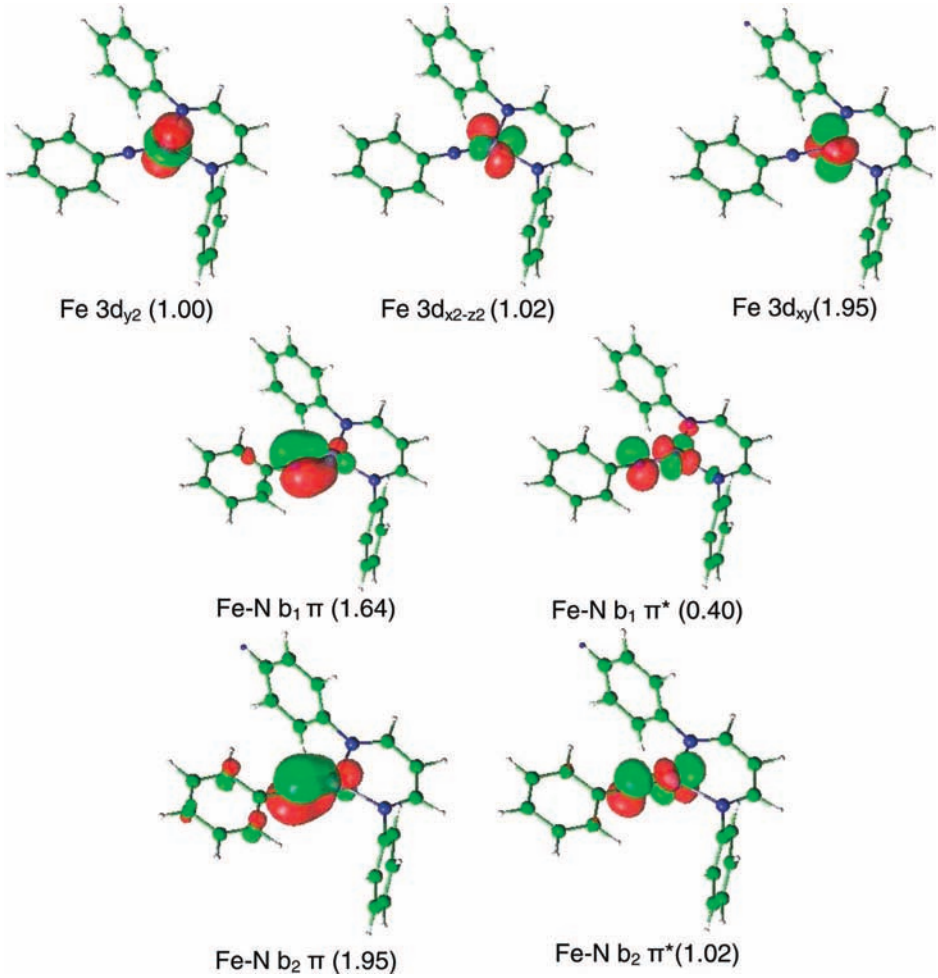

Figure 2. The active MOs of the Fe(III) complex (excluding the 4d orbitals). The occupation numbers (within parentheses) are for the 1 $^4B_2$ state. The contour line used is 0.05 e/au^3.

For four low-energy electronic states of each complex, we also carried out OLYP/TZP geometry optimizations and vibrational analyses. Zero-point energies were computed as well as selected thermodynamic functions at room temperature under the ideal gas approximation.

Single-point CASSCF[29] and CASPT2 calculations were carried out on the C_{2v} OLYP ground-state geometries using the MOLCAS-6 program system.[30,31] The basis set was of VDZP quality (VDZ for hydrogens), with the primitives obtained from the relativistic ANO-RCC basis set (Co 5s4p2d1f; C, N 3s2p1d; H 2s).[32] Thus, scalar relativistic effects are accounted for with the Douglas−Kroll−Hessian Hamiltonian, as is standard in the MOLCAS software.[33]

Different active spaces were tried and the final choice was to include the five metal 3d orbitals and the two imido p_π orbitals; three 4d orbitals, $d_{z^2}/d_{x^2-z^2}$, d_{xy}, and $d_{x^2-y^2}/d_{y^2}$, each of which is doubly occupied in at least two of the three complexes studied, were added to account for the "double shell effect".[34] This gives 10 active electrons in 10 orbitals for the Co(III) system, 9 in 10 for the Fe(III) and 11 in 10 for the Ni(III) system. Attempts to use a larger active space including the diiminato lone-pair orbitals failed because their occupation numbers remained very close to two and they preferred to be inactive.

Figures 2 and 3 depict the active MOs for the Fe(III) and Co(III) complexes, respectively. Note that the a_1-symmetry MOs have chosen different axes for the quantization of the angular momentum. In both systems, the two orbitals have the same occupation numbers (1.0 for Fe and 2.0 for Co), so it is only the summed density that matters, which should have the same qualitative topology in both systems. The active MOs of the Ni(III) complex (not shown) are very similar to those of the Fe(III) complex. Note that whereas the $d_{z^2}/d_{x^2-z^2}$ (a_1), $d_{x^2-y^2}/d_{y^2}$ (a_1) and d_{xy}-based MOs are largely metal-centered, the four b-symmetry π MOs are metal(d_π)−N_{imido}(p_π) in character; the bonding π MOs are referred to as b_2 and b_1, the corresponding antibonding ones as b_2* and b_1*. The Kohn–Sham MOs are also roughly the same shape as the CASSCF ones and are described hereafter with the same notation.

All valence electrons, including the metal 3s and 3p electrons, were correlated in the CASPT2 calculations, which employed the standard IPEA Hamiltonian and an imaginary level shift of 0.1 to remove some weak intruder states. Tables 1−3 present the CASPT2 energetics for the Fe(III), Co(III) and Ni(III) complexes; in general, two roots were calculated for each spin and each state symmetry.

Results

(a) Fe^{III}(diiminato)(NPh). According to Table 1, two nearly equienergetic quartets compete as contenders for the ground state of the Fe(III) complex. It is impossible to say definitively which one of these two is the actual ground state, even though all the DFT functionals examined favor the $^4B_2$ state by a couple of tenths of an eV, relative to the $^4B_1$ state. A quartet ground state is consistent with experimental EPR measurements in a related Fe^{III}(nacnac)(NAd) complex.[6] Moreover, the high-spin sextet

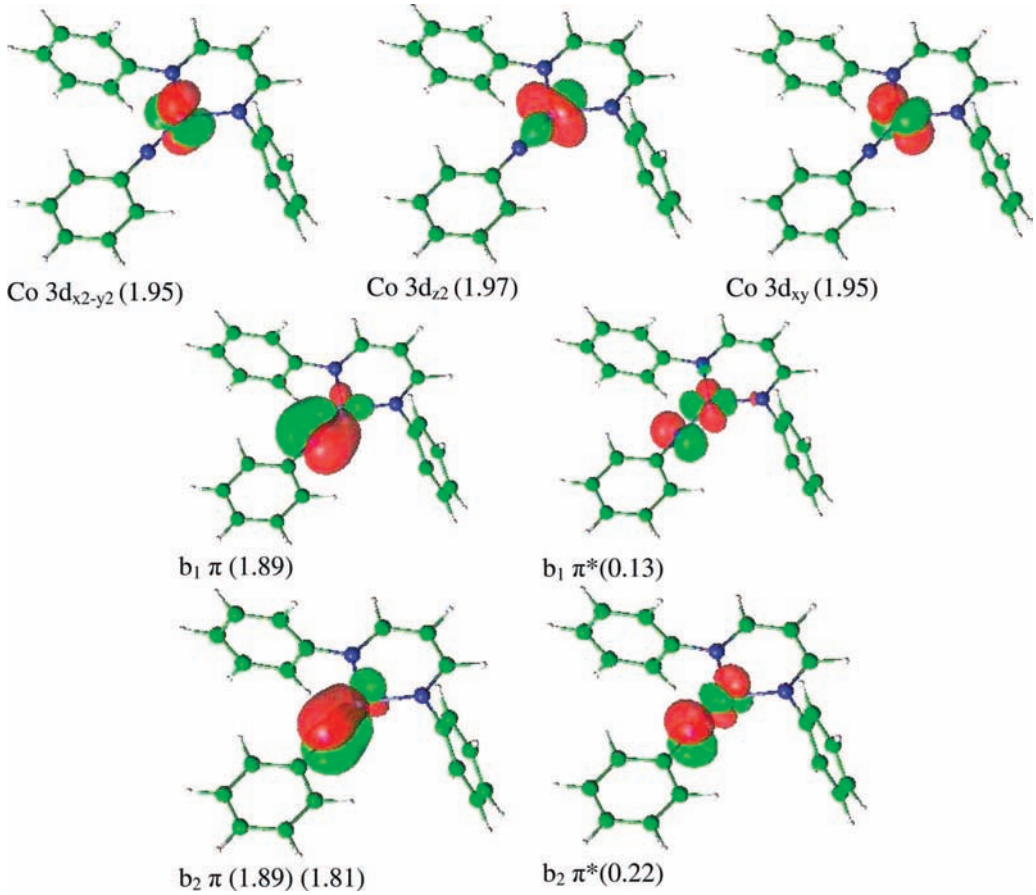

Figure 3. The active MOs of the Co(III) complex (excluding the 4d orbitals). The occupation numbers (within parentheses) are for the $^1A_1$ ground state. The contour line used is 0.05 e/au^3.

TABLE 1: Vertical CASPT2/VDZP Energies (eV) for the Two Lowest Quartet and Doublet States in Each Symmetry for the Fe^{III}(diiminato)(NPh) Complex[a]

state	configuration	energy (eV)
$1\ ^4B_2$	$(3d_{y^2})^1(3d_{x^2-z^2})^1(3d_{xy})^2(b_1)^2(b_2)^2(b_2^*)^1$	0.00
$1\ ^4B_1$	$3d_{xy} \rightarrow 3d_{y^2}$	0.07
$1\ ^6A_1$	$3d_{xy} \rightarrow b_1^*$	0.20
$2\ ^4B_2$	$3d_{xy}b_2^* \rightarrow 3d_{x^2-z^2}b_1^*$	0.31
$1\ ^2A_1$	$b_2^* \rightarrow 3d_{y^2}$	0.44
$2\ ^4B_1$	$3d_{xy} \rightarrow 3d_{x^2-z^2}$	0.47
$1\ ^2A_2$	$3d_{xy}b_2^* \rightarrow 3d_{y^2}3d_{x^2-z^2}$	0.55
$1\ ^6B_2$	$3d_{xy}b_2 \rightarrow 3d_{x^2-z^2}b_1^*$	1.20
$1\ ^2B_2$	$b_2^*(\uparrow) \rightarrow b_2^*(\downarrow)$ (spin flip)	1.28
$2\ ^2A_1$	$b_2^* \rightarrow 3d_{x^2-z^2}$	1.35
$1\ ^4A_1$	$3d_{xy} \rightarrow b_1^*$	1.39
$1\ ^2B_1$	$3d_{xy} \rightarrow 3d_{x^2-z^2}$	1.40
$1\ ^6B_1$	$3d_{xy}b_1 \rightarrow 3d_{x^2-z^2}b_1^*$	1.42
$2\ ^6B_1$	$b_2 \rightarrow b_1^*$	1.43
$2\ ^2B_1$	$3d_{xy} \rightarrow 3d_{y^2}$	1.62
$2\ ^2B_2$	$3d_{xy}b_2^* \rightarrow 3d_{x^2-z^2}b_1^*$	1.95
$2\ ^6B_2$	$3d_{xy}b_2 \rightarrow 3d_{y^2}b_1^*$	1.97
$1\ ^4A_2$	$3d_{xy}b_2 \rightarrow 3d_{y^2}3d_{x^2-z^2}$	2.14
$2\ ^4A_1$	$b_2 \rightarrow 3d_{x^2-z^2}$	2.14
$1\ ^6A_2$	$3d_{xy}b_1 \rightarrow b_1^*b_2^*$	2.31
$2\ ^6A_1$	$3d_{xy}b_2 \rightarrow b_1^*b_2^*$	2.87
$2\ ^2A_2$	$3d_{xy}b_2 \rightarrow 3d_{y^2}3d_{x^2-z^2}$	3.27
$2\ ^4A_2$	$b_2b_2^* \rightarrow 3d_{x^2-z^2}b_1^*$	3.52
$2\ ^6A_2$	$3d_{xy}b_2 \rightarrow b_1^*b_1^*$	3.66

[a] In addition, the high-spin $^6A_1$ state is also tabulated. The geometry assumed throughout is that obtained from an OLYP/STO-TZP optimization of the $^4B_2$ ground state.

TABLE 2: Vertical CASPT2/VDZP Energies (eV) for the Two Lowest Singlet, Triplet, and Quintet States in Each Symmetry for the Co^{III}(diiminato)(NPh) Complex[a]

state	configuration	energy (eV)
$1\ ^1A_1$	$(3d_{z^2})^2(3d_{x^2-y^2})^2(3d_{xy})^2(b_1)^2(b_2)^2$	0.00
$1\ ^3B_2$	$3d_{x^2-y^2} \rightarrow b_2^*$	0.11 (0.14)
$1\ ^3B_1$	$3d_{xy} \rightarrow b_2^*$	0.15 (0.50[b])
$2\ ^3B_1$	$3d_{z^2} \rightarrow b_1^*$	0.52 (0.50)
$1\ ^5A_1$	$3d_{z^2}3d_{xy} \rightarrow b_1^*b_2^*$	0.59 (0.61)
$1\ ^5A_2$	$3d_{x^2-y^2}3d_{z^2} \rightarrow b_1^*b_2^*$	0.59 (0.53)
$2\ ^3B_2$	$3d_{xy} \rightarrow b_1^*$	0.65
$1\ ^1B_2$	$3d_{x^2-y^2} \rightarrow b_2^*$	0.83 (0.82)
$1\ ^1B_1$	$3d_{xy} \rightarrow b_2^*$	0.84 (0.84)
$1\ ^3A_1$	$3d_{z^2}3d_{x^2-y^2} \rightarrow (b_2^*)^2$	0.96 (0.99)
$1\ ^3A_2$	$3d_{x^2-y^2}3d_{xy} \rightarrow (b_2^*)^2$	1.04 (1.35)
$2\ ^1B_2$	$0.73(3d_{z^2} \rightarrow b_2^*) - 0.51(3d_{xy} \rightarrow b_1^*)$	1.07
$2\ ^3A_2$	$3d_{z^2}3d_{x^2-y^2} \rightarrow b_1^*b_2^*$	1.35
$2\ ^3A_1$	$3d_{z^2}3d_{xy} \rightarrow b_1^*b_2^*$	1.48
$2\ ^1B_1$	$3d_{x^2-y^2} \rightarrow b_1^*$	1.52
$2\ ^5A_1$	$3d_{x^2-y^2}3d_{xy} \rightarrow b_1^*b_2^*$	1.54
$1\ ^5B_1$	$3d_{x^2-y^2}b_2 \rightarrow b_1^*b_2^*$	1.71 (1.64)
$1\ ^5B_2$	$3d_{x^2-y^2}b_1 \rightarrow b_1^*b_2^*$	1.89 (1.86)
$2\ ^5B_2$	$3d_{xy}b_2 \rightarrow b_1^*b_2^*$	1.91
$2\ ^5B_1$	$3d_{xy}b_1 \rightarrow b_1^*b_2^*$	2.00
$2\ ^5A_2$	$3d_{z^2}3d_{xy}b_1 \rightarrow b_1^*(b_2^*)^2$	2.56
$1\ ^1A_2$	$b_1 \rightarrow b_2^*$	3.14 (3.91)*
$2\ ^1A_1$	$0.61(b_1 \rightarrow b_1^*) + 0.56(b_2 \rightarrow b_2^*)$	3.47
$2\ ^1A_2$	$b_2 \rightarrow b_1^*$	3.90

[a] The geometry assumed throughout is that obtained from an OLYP/TZP optimization of the $^1A_1$ ground state. Energy values within parentheses were obtained from single-root calculations. [b] The single root calculation converged to a different root.

TABLE 3: Vertical CASPT2/VDZP Energies (eV) for the Two Lowest Doublet and Quartet States in Each Symmetry for the Ni^{III}(diiminato)(NPh) Complex[a]

state	configuration	energy (eV)
$1\ ^2B_2$	$(3d_{y^2})^2(3d_{x^2-z^2})^2(3d_{xy})^2(b_1)^2(b_2)^2(b_2^*)^1$	0.00
$1\ ^2B_1$	$b_2^* \rightarrow b_1^*$	0.40
$1\ ^4A_2$	$3d_{y^2} \rightarrow b_1^*$	0.72
$2\ ^4A_2$	$3d_{x^2-z^2} \rightarrow b_1^*$	0.79
$1\ ^4A_1$	$3d_{xy} \rightarrow b_2$	0.86
$1\ ^2A_1$	$3d_{x^2-z^2} \rightarrow b_2^*$	0.87
$1\ ^2A_2$	$3d_{xy} \rightarrow b_2^*$	0.99
$2\ ^2A_1$	$3d_{y^2} \rightarrow b_2^*$	1.22
$2\ ^2A_2$	$3d_{x^2-z^2}b_2 \rightarrow b_1^*b_2^*$	1.26
$1\ ^4B_1$	$b_2 \rightarrow b_1^*$	1.45
$1\ ^4B_2$	$b_1 \rightarrow b_1^*$	1.67
$2\ ^2B_2$	$b_2 \rightarrow b_2^*$	1.89
$2\ ^4A_1$	$3d_{x^2-z^2}b_1 \rightarrow b_1^*b_2^*$	2.21
$2\ ^4B_1$	$3d_{y^2}3d_{x^2-z^2} \rightarrow b_1^*b_2^*$	2.34
$2\ ^4B_2$	$3d_{y^2}3d_{xy} \rightarrow b_1^*b_2^*$	2.47
$2\ ^2B_1$	$b_1 \rightarrow b_2^*$	2.90

[a] The geometry assumed throughout is that obtained from an OLYP/TZP optimization of the $^2B_2$ ground state.

($^6A_1$ at 0.20 eV), two additional quartets ($2\ ^4B_2$ at 0.31 eV), and even a low-spin doublet ($1\ ^2A_1$ at 0.44 eV) all occur at rather low energies, <0.5 eV, relative to the ground state.

From a one-electron perspective, the near-degeneracy of the two lowest quartet states reflects the near-degeneracy of the d_{y^2}, $d_{x^2-z^2}$, and d_{xy} orbitals. By comparison, the π^* Kohn–Sham orbitals, b_2^* and b_1^*, are distinctly, but by no means very much, higher in energy, with b_1^* somewhat higher in energy than b_2^*. As noted previously,[8] this MO ordering holds across all diiminato−imido complexes examined to date. Again, from a one-electron perspective, the overall dense phalanx of d−d excited states shown in Table 1 follows from the more or less close spacing of all the Fe 3d-based MOs.

(b) Co^{III}(diiminato)(NPh). For Co(III), the $S = 0$ ground state (see Table 2) of our model complex is consonant with that observed experimentally for a closely related Co^{III}(nacnac)(NAd) complex.[2] However, once again, there are two exceedingly low-lying excited states ($1\ ^3B_1$ (0.11 eV) and $1\ ^3B_1$ (0.15 eV)) and, on the basis of the CASPT2 energetics alone, we cannot predict which of the three lowest states is the actual ground state. As in the Fe(III) case, the near-degeneracy of these two excited states reflects the near-degeneracy of the d_{y^2}, $d_{x^2-z^2}$, and d_{xy} orbitals.

Besides the three states mentioned above, there are no other particularly low-lying states. The lowest quintets are around 0.6 eV relative to the ground state. Additional triplet states also occur above 0.5 eV. In a one-electron picture, these results indicate that the b_1^* MO has a considerably higher orbital energy than the b_2^*. The reason for this, as noted before,[1,2,6,8] is that the b_1^* MO is destabilized by σ-antibonding interactions involving the diiminato ligand.

(c) Ni^{III}(diiminato)(NPh). In contrast to the Fe(III) and Co(III) cases, the Ni(III) complex exhibits a clearly nondegenerate ground state, $^2B_2$, which corresponds to a $(3d_{y^2})^2(3d_{x^2-z^2})^2(3d_{xy})^2(b_1)^2(b_2)^2(b_2^*)^1$ configuration.[35] According to Table 3, the alternative $(b_1^*)^1$ doublet is higher in energy by quite a substantial margin of energy (0.4 eV). Relative to the two lowest-energy doublets, the lowest quartets are again significantly higher in energy; thus, there are three quartet states between 0.7 and 0.9 eV, relative to the ground state.

Discussion

On the basis of unpublished work in our laboratories (where we compared CASPT2 spin-state energetics obtained with VDZP and VTZP basis sets),[36] we believe that the energetics results reported in Tables 1−3 are converged to within about 0.2 eV of the basis set limit. These results, therefore, may be viewed as benchmarks against which we may evaluate the performance of different functionals. Tables 4−6 compare the relative energies of a number of low-energy spin states for the three metal complexes studied, for CASPT2 and a number of commonly used exchange-correlation functionals. The main conclusions are as follows.

TABLE 4: Comparison of CASPT2 and DFT Energetics (eV) for Several Low-Energy Spin States of the Fe^{III}(diiminato)(NPh) Complex Studied

		CASPT2	DFT (STO-TZP)						
state	configuration	VDZP	OLYP	OPBE	BLYP	PW91	BP86	B3LYP	B3LYP*
$1\ ^4B_2$	$(3d_{y^2})^1(3d_{x^2-z^2})^1(3d_{xy})^2\ (b_1)^2(b_2)^2(b_2^*)^1$	0.00	0.00	0.00	0.00	0.00	0.00	0.00	0.00
$1\ ^4B_1$	$3d_{xy} \rightarrow 3d_{y^2}$	0.07	0.29	0.34	0.25	0.28	0.28	0.16	0.18
$2\ ^4B_2$	$3d_{xy}b_2^* \rightarrow 3d_{x^2-z^2}b_1^*$	0.31	0.80	0.87	0.84	0.88	0.87	0.42	0.54
$1\ ^2A_1$	$b_2^* \rightarrow 3d_{y^2}$	0.44	0.37	0.52	0.04	0.15	0.15	[a]	0.27
$1\ ^2A_2$	$3d_{xy}b_2^* \rightarrow 3d_{y^2}3d_{x^2-z^2}$	0.55	0.75	0.93	[a]	0.50	0.51	0.53	0.51
$1\ ^6A_1$	$3d_{xy} \rightarrow b_1^*$	0.20	0.79	0.70	1.15	1.07	1.05	0.58	0.69
rms deviation relative to CASPT2		0.00	0.34	0.36	0.52	0.45	0.44	0.18	0.26

[a] These calculations could not be converged.

TABLE 5: Comparison of CASPT2 and DFT Energetics (eV) for Several Low-Lying Spin States of the Co^{III}(diiminato)(NPh) Complex Studied

		CASPT2	DFT (STO-TZP)						
state	configuration	VDZP	OLYP	OPBE	BLYP	PW91	BP86	B3LYP	B3LYP*
$1\ ^1A_1$	$(3d_{z^2})^2(3d_{x^2-y^2})^2(3d_{xy})^2\ (b_1)^2(b_2)^2$	0.00	0.00	0.00	0.00	0.00	0.00	0.00	0.00
$1\ ^3B_2$	$3d_{x^2-y^2} \rightarrow b_2^*$	0.11	0.31	0.19	0.52	0.44	0.43	−0.09	0.07
$1\ ^3B_1$	$3d_{xy} \rightarrow b_2^*$	0.15	0.60	0.55	0.70	0.67	0.66	0.06	0.23
$2\ ^3B_1$	$3d_{z^2} \rightarrow b_1^*$	0.52	0.88	0.82	1.08	1.04	1.03	0.24	0.51
$2\ ^3B_2$	$3d_{xy} \rightarrow b_1^*$	0.65	1.35	1.31	1.50	1.46	1.45	0.54	0.83
$1\ ^5A_2$	$3d_{x^2-y^2}3d_{z^2} \rightarrow b_1^*b_2^*$	0.59	1.01	0.84	1.47	1.35	1.34	0.33	0.63
$1\ ^5A_1$	$3d_{z^2}3d_{xy} \rightarrow b_1^*b_2^*$	0.59	1.19	1.06	1.63	1.53	1.51	0.47	0.77
rms deviation relative to CASPT2		0.00	0.45	0.37	0.69	0.63	0.62	0.19	0.10

TABLE 6: Comparison of Selected CASPT2 and DFT Vertical Excitation Energies (eV) for the Ni^{III}(diiminato)(NPh) Complex Studied

state	configuration	CASPT2 VDZP	DFT (STO-TZP) OLYP	OPBE	BLYP	PW91	BP86	B3LYP	B3LYP*
$1\ ^2B_2$	$(3d_{y^2})^2(3d_{x^2-z^2})^2(3d_{xy})^2\ (b_1)^2(b_2)^2(b_2^*)^1$	0.00	0.00	0.00	0.00	0.00	0.00	0.00	0.00
$1\ ^2B_1$	$b_2^* \rightarrow b_1^*$	0.40	0.69	0.70	0.69	0.70	0.70	0.43	0.55
$1\ ^2A_1$	$3d_{x^2-z^2} \rightarrow b_2^*$	0.87	1.55	1.49	1.66	1.63	1.63	1.09	1.28
$1\ ^4A_2$	$3d_{y^2} \rightarrow b_1^*$	0.72	1.04	0.99	1.26	1.22	1.22	0.64	0.83
$1\ ^4A_1$	$3d_{xy} \rightarrow b_2$	0.79	1.54	1.51	1.65	1.63	1.62	0.88	1.08
	rms deviation relative to CASPT2	0.00	0.49	0.46	0.59	0.57	0.57	0.11	0.24

TABLE 7: Relative Electronic Energies E_{rel}, Thermodynamic Energies (U_{rel})[b] or Enthalpies (H_{rel}),[c] and Relative Gibbs Free Energies (G_{rel}) Based on OLYP/STO-TZP Geometries and Harmonic Frequencies and the Ideal Gas Approximation at 298.15 K[a]

system	state	configuration	E_{rel}	U_{rel}/H_{rel}	G_{rel}
Fe(III)	$1\ ^4B_2$	$(3d_{y^2})^1(3d_{x^2-z^2})^1(3d_{xy})^2\ (b_1)^2(b_2)^2(b_2^*)^1$	**0.00 (0.00)**	**0.00 (0.00)**	**0.00 (0.00)**
Fe(III)	$1\ ^4B_1$	$3d_{xy} \rightarrow 3d_{y^2}$	5.72 (0.25)	5.82 (0.25)	5.61 (0.24)
Fe(III)	$2\ ^4B_2$	$3d_{xy}b_2^* \rightarrow 3d_{x^2-z^2}b_1^*$	12.23 (0.53)	10.56 (0.46)	13.12 (0.57)
Fe(III)	$1\ ^2A_1$	$b_2^* \rightarrow 3d_{y^2}$	6.87 (0.30)	7.27 (0.31)	8.30 (0.36)
Co(III)	$1\ ^1A_1$	$(3d_{z^2})^2(3d_{x^2-y^2})^2(3d_{xy})^2\ (b_1)^2(b_2)^2$	**0.00 (0.00)**	**0.00 (0.00)**	**0.00 (0.00)**
Co(III)	$1\ ^3B_2$	$3d_{x^2-y^2} \rightarrow b_2^*$	5.38 (0.23)	4.96 (0.21)	4.43 (0.19)
Co(III)	$1\ ^3B_1$	$3d_{xy} \rightarrow b_2^*$	10.67 (0.46)	10.17 (0.44)	9.29 (0.40)
Co(III)	$2\ ^3B_1$	$3d_{z^2} \rightarrow b_1^*$	13.90 (0.60)	11.78 (0.51)	12.84 (0.56)
Ni(III)	$^2B_2$	$(3d_{y^2})^2(3d_{x^2-z^2})^2(3d_{xy})^2\ (b_1)^2(b_2)^2(b_2^*)^1$	**0.00 (0.00)**	**0.00 (0.00)**	**0.00 (0.00)**
Ni(III)	$^2B_1$	$b_2^* \rightarrow b_1^*$	14.96 (0.65)	13.99 (0.61)	14.92 (0.65)
Ni(III)	$^4A_2$	$3d_{y^2} \rightarrow b_1^*$	19.29 (0.84)	16.71 (0.72)	19.11 (0.83)
Ni(III)	$^4A_1$	$3d_{x^2-z^2} \rightarrow b_2^*$	29.97 (1.30)	28.98 (1.26)	29.89 (1.30)

[a] All energies shown are in kcal/mol (eV). The energy zero level for each system is indicated in bold. [b] The thermodynamic energy U is the sum of the electronic energy E, the zero-point energy, and translational, vibrational and rotational energies at 298.15 K. [c] Trends in U_{rel} and H_{rel} are identical because the work term RT in the latter cancels out.

As far as the Fe(III) complex is concerned, the various functionals examined all seem to perform "tolerably", the rms deviations relative to CASPT2 energies ranging from 0.18 to 0.52 eV (see Table 4), though none can be described as performing well. For the $2\ ^4B_2$ state, for example, all the pure functionals examined predict unduly high energies relative to CASPT2; the hybrid functionals are better, B3LYP being somewhat better than B3LYP*. For the $^6A_1$ state, which is only 0.2 eV above the ground state at the CASPT2 level, all the functionals appear to perform badly, greatly exaggerating the energy of the state, the classic pure functionals being the worst.

For the Co(III) system, all the pure functionals examined fail to predict low-energy triplet states. However, B3LYP and B3LYP* do do so. B3LYP seems to have a tendency to unduly stabilize higher-spin states.[15] For example, B3LYP predicts an $S = 1$ state as the lowest-energy state, albeit by a small margin of energy. As far as the quintet states are concerned, the pure functionals again greatly exaggerate their energy. B3LYP and B3LYP* are much better, yielding energies in good agreement with CASPT2.

The same pattern is seen for the Ni(III) complex. In other words, the pure functionals greatly overestimate the energies of the high-spin quartet states; B3LYP and B3LYP* are much better. Overall, unlike in certain other studies,[13–15] B3LYP, rather than B3LYP*, clearly emerges as the best functional, relative to CASPT2 benchmarks.

Finally, Table 7, where we list OLYP thermodynamic energies/enthalpies and free energies for the four lowest states of each system, shows that the trends in these quantities are very much the same as those in the pure electronic energies. For our purposes, therefore, the data in Tables 1−6 appear to be entirely adequate.

We conclude on a cautionary note. Although this study seems to reinforce the view that hybrid functionals are better than pure functionals, transition metal complexes afford a host of counterexamples.[13,15] In a recent study of the spin-crossover complex Fe(salen)(NO),[13] for instance, we found that only the newer pure functionals OLYP and OPBE, based on the OPTX exchange functional, and the B3LYP* hybrid functional, which has a reduced amount (15%) of Hartree–Fock exchange relative to B3LYP (20%), correctly capture the observed spin-crossover behavior; in other words, only these functionals predict equienergetic doublet and quartet states for this complex. B3LYP, in contrast, predicts a quartet ground state. Accordingly, on the basis of this study, we cannot claim to have identified the best exchange-correlation functional for transition metal complexes in general. However, we trust that we have demonstrated the value of ab initio CASPT2 calculations and of DFT/ab initio calibration studies vis-à-vis the issue of transition metal spin-state energetics.

Acknowledgment. A.G. acknowledges partial support from the Research Council of Norway. B.O.R. acknowledges financial support by the Swedish Research Council (VR) through the Linnaeus Center of Excellence on Organizing Molecular Matter (OMM).

Supporting Information Available: Optimized Cartesian coordinates for selected ground-state structures. This material is available free of charge via the Internet at http://pubs.acs.org.

References and Notes

(1) Mehn, M. P.; Peters, J. C. *J. Inorg. Biochem.* **2006**, *100*, 634–643.
(2) Dai, X.; Kapoor, P.; Warren, T. H. *J. Am. Chem. Soc.* **2004**, *126*, 4798–4799.

(3) Jenkins, D. M.; Di Bilio, A. J.; Allen, M. J.; Betley, T.; Peters, J. C. *J. Am. Chem. Soc.* **2002**, *124*, 15336–15350.

(4) Hu, X.; Meyer, K. *J. Am. Chem. Soc.* **2004**, *126*, 16322–16323.

(5) Cowley, R. E.; Bontchev, R. P.; Sorrell, J.; Sarracino, O.; Feng, Y.; Wang, H.; Smith, J. M. *J. Am. Chem. Soc.* **2007**, *129*, 2424–2425.

(6) Eckart, N. A.; Vaddadi, S.; Stoian, S.; Lachicotte, R. J.; Cundari, T. R.; Holland, P. L. *Angew. Chem., Int. Ed.* **2006**, *45*, 6868–6871.

(7) Tangen, E.; Conradie, J.; Ghosh, A. *J. Chem. Theory Comput.* **2007**, *3*, 448–457.

(8) Conradie, J.; Ghosh, A. *J. Chem. Theory Comput.* **2007**, *3*, 689–702.

(9) Wasbotten, I. H.; Ghosh, A. *Inorg. Chem.* **2007**, *46*, 7890–7898.

(10) (a) Shay, D. T.; Yap, G. P. A.; Zakharov, L. N.; Rheingold, A. L.; Theopold, K. H. *Angew. Chem., Int. Ed.* **2005**, *44*, 1508–1510. (b) Corrigendum: Shay, D. T.; Yap, G. P. A.; Zakharov, L. N.; Rheingold, A. L.; Theopold, K. H. *Angew. Chem. Int. Ed* **2006**, *45*, 7870–7870.

(11) Selected studies comparing the performance of different functionals vis-à-vis transition metal spin-state energetics: (a) Ghosh, A.; Persson, B. J.; Taylor, P. R. *J. Biol. Inorg. Chem.* **2003**, *8*, 507–511. (b) Swart, M.; Groenhof, A. R.; Ehlers, A. W.; Lammertsma, K. *J. Phys. Chem. A* **2004**, *108*, 5479–5483. (c) Swart, M.; Ehlers, A. W.; Lammertsma, K. *Mol. Phys.* **2004**, *102*, 2467–2474. (d) Deeth, R. J.; Fey, N. *J. Comput. Chem.* **2004**, *25*, 1840–1848. (e) Groenhof, A. R.; Swart, M.; Ehlers, A. W.; Lammertsma, K. *J. Phys. Chem. A* **2005**, *109*, 3411–3417. (f) Daku, L. M. L.; Vargas, A.; Hauser, A.; Fouqueau, A.; Casida, M. E. *ChemPhysChem* **2005**, *6*, 1393–1410. (g) Ganzenmuller, G.; Berkaine, N.; Fouqueau, A.; Casida, M. E.; Reiher, M. *J. Chem. Phys.* **2005**, *122*, Art. No. 234321. (h) De Angelis, F.; Jin, N.; Car, R.; Groves, J. T. *Inorg. Chem.* **2006**, *45*, 4268–4276. (i) Vargas, A.; Zerara, M.; Krausz, E.; Hauser, A.; Daku, L. M. L. *J. Chem. Theory Comput.* **2006**, *2*, 1342–1359. (j) Rong, C. Y.; Lian, S. X.; Yin, D. L.; Shen, B.; Zhong, A. G.; Bartolotti, L.; Liu, S. B. *J. Chem. Phys.* **2006**, *125*, Art. No. 174102. (k) Strickland, N.; Harvey, J. N. *J. Phys. Chem. B* **2007**, *111*, 841–852. (l) Conradie, J.; Ghosh, A. *J. Phys. Chem. B* **2007**, *111*, 12621–12624.

(12) Andersson, K.; Malmqvist, P.-Å.; Roos, B. O. *J. Chem. Phys.* **1992**, *96*, 1218–1226.

(13) Ghosh, A.; Taylor, P. R. *Curr. Opin. Chem. Biol.* **2003**, *91*, 113–124.

(14) Harvey, J. N. *Struct. Bonding (Berlin)* **2004**, *112*, 151–183.

(15) Ghosh, A. *J. Biol. Inorg. Chem.* **2006**, *11*, 712–724.

(16) (a) Perdew, J. P.; Chevary, J. A.; Vosko, S. H.; Jackson, K. A.; Perderson, M. R.; Singh, D. J.; Fiolhais, C. *Phys. Rev. B* **1992**, *46*, 6671–6687. (b) Erratum. Perdew, J. P.; Chevary, J. A.; Vosko, S. H.; Jackson, K. A.; Perderson, M. R.; Singh, D. J.; Fiolhais, C. *Phys. Rev. B* **1993**, *48*, 4978.

(17) Becke, A. D. *Phys. Rev.* **1988**, *A38*, 3098.

(18) Lee, C.;. Yang, W.; Parr, R. G. *Phys. Rev.* **1988**, *B37*, 785–789.

(19) (a) Perdew, J. P. *Phys. Rev.* **1986**, *B33*, 8822. (b) Erratum Perdew, J. P. *Phys. Rev.* **1986**, *B34*, 7406.

(20) Watson, M. A.; Handy, N. C.; Cohen, A. J. *J. Chem. Phys.* **2003**, *119*, 6475–6481.

(21) Stephens, J. Devlin, F. J.; Chabalowski, C. F.; Frisch, M. J. *J. Phys. Chem.* **1994**, *98*, 11623–11627.

(22) Hertwig, R. H.; Koch, W. *Chem. Phys. Lett.* **1997**, *268*, 345–351.

(23) The OLYP functional is based on the OPTX exchange functional: Handy, N. C.; Cohen, A. J. *Mol. Phys.* **2001**, *99*, 403–412. The correlation functional is LYP.[18]

(24) Throughout this paper, the irreducible representations refer to the C_{2v} point group.

(25) The ADF program system was obtained from Scientific Computing and Modeling, Amsterdam (http://www.scm.com/). For a description of the methods used in ADF, see: Velde, G. T.; Bickelhaupt, F. M.; Baerends, E. J.; Guerra, C. F.; Van Gisbergen, S. J. A.; Snijders, J. G.; Ziegler, T. *J. Comput. Chem.* **2001**, *22*, 2001.

(26) Perdew, J. P.; Burke, K.; Ernzerhof, M. *Phys. Rev. Lett.* **1996**, *77*, 3865–3868.

(27) Perdew, J. P.; Burke, K.; Ernzerhof, M. *Phys. Rev. Lett.* **1997**, *7*, 8–1396.

(28) Reiher, M.;. Salomon, O.; Hess, B. A. *Theor. Chem. Acc.* **2001**, *107*, 48.

(29) Roos, B. O. *Adv. Chem. Phys.* **1987**, *69*, 399–445.

(30) Karlström, G.; Lindh, R.; Malmqvist, P.-Å.; Roos, B. O.; Ryde, U.; Veryazov, V.; Widmark, P.-O.; Cossi, M.; Schimmelpfennig, B.; Neogrady, P.; Seijo, L. *Comput. Mater. Sci.* **2003**, *28*, 222.

(31) The fact that we have used ground-state OLYP geometries in all calculations is worth commenting upon. Several considerations prompted us to choose this course of action. First, geometry optimizations, frequency calculations, and hence estimations of zero-point energy effects are currently not possible at the CASPT2 level. Second, we found in the course of an earlier study of diiminato−imido complexes that the errors in fixed geometry studies, relative to those involving optimization of each excited state, are generally on the order of 0.1 eV. Third, ground-state DFT methods are applicable to only a small subset of states that we have calculated with CASPT2. Overall, the DFT/CASPT2 comparison carried out here is necessarily inexact, but sufficiently accurate, we believe, to be useful.

(32) Roos, B. O.; Lindh, R.; Malmqvist, P.-Å.; Veryazov, V.; Widmark, P.-O. *J. Phys. Chem. A* **2005**, *109*, 6575.

(33) (a) Douglas, M.; Kroll, N. M. *Ann. Phys.* **1974**, *82*, 89–155. (b) Hess, B. A. *Phys. Rev.* **1986**, *A33*, 3742–3748.

(34) Andersson, K.; Roos, B. O. *Chem. Phys. Lett.* **1992**, *191*, 507–514.

(35) Kogut, E.; Wiencko, H. L.; Zhang, L. B.; Cordeau, D. E.; Warren, T. H. *J. Am. Chem. Soc.* **2005**, *127*, 11248–11249.

(36) Aquilante, F.; Malmqvist, P.-Å.; Pedersen, T. B.; Ghosh, A.; Roos, B. O. *J. Chem. Theory Comput.* **2008**, *4*, 694−702.

JP711159H